REVISION TO MANUSCRIPT DRAFT

Wind Energy Science Discussion

Comparison between upwind and downwind designs of a 10 MW wind turbine rotor

The authors would like to thank the two reviewers for their time and for the useful feedback. All provided input indeed contributes to the improvement of the paper.

A list of point-by-point replies to the reviewers' comments is reported in the following.

Reviewer #1

Numbered comments

1. *[**Reviewer**] Can you explain why this blockage effect is favorable, with respect to power/loads?*

   [**Authors**] The benefit is claimed by Kress et al., 2015[1], and it refers to AEP. This increase is explained by a redirection of the flow towards the outboard part of the blade due to the presence of the nacelle located upwind. The flow speeds up towards blade sections characterized by thinner and more efficient airfoils and, as a result, a higher AEP is produced. An experimental campaign on sub-scale models showed an increase in AEP equal to 5% against an increase of 3% of rotor thrust. A similar concept is behind GE's ecoROTR[2]. The actual benefit in full-scale wind turbines is yet to be investigated. Research activities within IEA Wind Task 40 aim at a more precise quantification of the potential benefits.

   The text in Sect. 1 was modified to incorporate the above comments.

2. *[**Reviewer**] How the AEP has been computed, how large is the uncertainty. 0.7% seems to be small compared to the uncertainty in the calculation*

   [**Authors**] It is true that a variation of 0.7% may look small, especially when subjected to a variety of uncertainties such as in the case of wind turbine simulation. Nonetheless, it should be remarked that a variation in the AEP of 0.7% between two rotors characterized by the same rotor diameter, both optimized in terms of twist and control, both of class I (where the contribution of region III to AEP is not marginal) and both subjected to the same wind is not negligible. In addition, the trend is consistent between the rotors with the baseline diameter (UW vs DW) and the rotors with the longer blades (UW5 vs DW5). Finally, tests computed with steady-state wind conditions corroborate the results.

   The text in Sect. 3.3 was modified to better support the claim of the 0.7% increase in AEP.

[1] Kress C, Chokani N, Abhari RS. Downwind wind turbine yaw stability and performance. Renewable Energy, 2015;83:1157-1165. doi: 10.1016/j.renene.2015.05.040

[2] https://www.ge.com/reports/post/126500095500/the-road-to-ecorotr-how-building-a-better-wind-2/

3. *[**Reviewer**] Activity*

   [**Authors**] The misprint was corrected.

General comments

1. *[**Reviewer**] Please describe in more details the assumption in the simulation study, for example in the wind regime, turbulence intensity, wind shear*

   [**Authors**] All simulations respected the IEC guidelines. Text is added at the beginning of Sect. 3.1 to briefly explain each Design Load Case (DLC) and to refer to the IEC standards.

2. *[**Reviewer**] How many seeds have been used to generate the turbulence inflow, is the number large enough to support the 0.7% AEP increase stated in the paper*

   [**Authors**] As stated in Sect. 3.1, only one turbulence seed was used to limit computational costs. Including more seeds would certainly produce some variations in the figure of 0.7% but would not change the trends shown in the paper. The consistency in the increase of the AEP is confirmed by simulations performed with a steady-state wind.

   Text was adjusted in Sect. 3.1 to better explain this point, and in Sect. 4 with a recommendation to run in the future the full load analysis as prescribed by the international standards.

3. *[**Reviewer**] What kind of tower shadow model has been used for the downwind case*

   [**Authors**] The tower shadow is computed based on an empirical model described in Powles, 1983[3]. This approach models the wake behind the tower using Δ, which is the maximum velocity deficit at the center of the wake as a fraction of the local wind speed, and W, which is the width of the tower shadow as a proportion of the local tower diameter. These quantities are defined for a given downwind distance, expressed as a proportion of the local tower diameter. For other distances, W increases, and Δ decreases, with the square root of the distance.

   The reference to the model was added in Sect. 2.1 of the paper.

4. *[**Reviewer**] How large is the uncertainty of the blade cost model of Sandia. Will the uncertainties increase the model is used for 10 MW wind turbine blade, for which the cost model is not calibrated.*

   [**Authors**] The SANDIA blade cost model, such as any cost model available in the public domain, is affected by a multitude of uncertainties. Nonetheless, conclusions similar to the ones reported in the paper would be drawn by looking at physical quantities such as blade mass and AEP. This is indeed the main reason why these quantities are reported in Fig. 4 together with blade cost and CoE. A note in this sense was added to the text.

[3] Powles SRJ. The effects of tower shadow on the dynamics of a HAWT. Wind Engineering, 7, 1983.

5. *[**Reviewer**] Using active coning will introduce uncertainty in the cone angles, meaning each of the blades may have slightly different cone angle. How would that impact the loads?*

   [**Authors**] A misalignment in the individual cone angles of the three blades would be extremely problematic generating mass and load imbalances to the whole turbine system. This is the main reason why individual flapping is not included in the present work, as explained in Section 2.3. It is nonetheless true that even with collective flapping, some misalignment could occur and would be a major concern.

   This aspect was added to Sect. 3.4, which discusses the critical aspects of DW5LA.

6. *[**Reviewer**] What is the impact of downwind configuration on the tower loads*

   [**Authors**] The ultimate and fatigue fore-aft moments measured at tower base were added to Figure 4. A discussion on the loads at tower base was added to Sect. 3.3. This comment is indeed very useful, as fatigue loads on the tower do experience an increase of a few percent points for configurations DW and DW5.

7. *[**Reviewer**] Will pitch activities of downwind turbine increase turbulence?*

   [**Authors**] In this study, downwind rotors are not characterized by a more pronounced pitching activity compared to the equivalent upwind designs. Therefore, we do not expect a special effect on turbulence due to pitching in a downwind turbine.

8. *[**Reviewer**] Complex terrain is not just an upflow angle, often flow characteristics may have also significant impacts on the loads*

   [**Authors**] This is absolutely true. The present paper does not however recommend complex terrain as a solution compared to flat terrains. The paper rather claims that downwind rotors may offer superior performance compared to upwind configurations in sites characterized by upflow conditions. More detailed studies should investigate the impact of loads due to unsteady inflow in complex terrains. This aspect was added in Sect. 4.2 among the recommendations for future work.

Reviewer #2

1. *[**Reviewer**]: As acknowledged by the authors, one critical parameter of the aerodynamic analysis of downwind rotors is the modeling of the blade tower interference. The authors mention that the model used in the analysis of the downwind configuration differs from the one used in the analysis of upwind rotors. It would be nice to comment on the validity of this model. A short comment and a reference to some earlier development would be sufficient as the above model could be critical for the consistent prediction of the fatigue loads, especially in the wind speeds range where coning is not activated.*

   [**Authors**] This aspect is pointed out by both reviewers, see point 3 of the General Comments of Reviewer 1. A specific reference (Powles, 1983) was added to Sect. 2.1.

2. *[**Reviewer**] In the same direction, it is mentioned that nacelle anemometer wind speed measurements are inaccurate and therefore some rotor equivalent wind speed could be estimated (most probably based on loads measurements if I'm not mistaken). It would be nice to provide an estimate of the uncertainty of the wind measurement if such a method is applied (I guess/hope that this uncertainty decreases as higher frequencies of turbulence are filtered out). Has this uncertainty been taken into account in the control loop of the active cone or you have considered perfect wind speed measurements?*

   [**Authors**] In this study we have not integrated the rotor measurements to predict the wind speed, but we rather assumed point measurements at the nacelle top.

   The comment of the reviewer is however interesting, as it highlights the importance of more precise measurements of the wind and how this increased accuracy may differently impact different rotor configurations. The authors will keep this suggestion for future work in consideration.

3. *[**Reviewer**] It is not perfectly understood how the radius of the blade was extended. Was that done by increasing the length of the blade or by increasing the radius of the hub keeping the same blade length? If the length of the blade is changed how the planform was scaled up?*

   [**Authors**] For configurations UW5 and DW5, the hub is left untouched and the blade planform is stretched. The twist is then re-optimized to ensure good airfoil efficiency along blade span. At this point, loads are re-computed and the blade internal structure is re-sized.

   Such approach is chosen thanks to its simplicity, in contrast to a full aero-structural optimization process. It is true that this choice may introduce some penalty in the design of the longer blades mounted on the UW5 and DW5 configurations. To alleviate this issue, the comparisons have indeed been mostly conducted between UW and DW as well as among UW5, DW5 and DW5LA, where the penalty, if any, affects the blades in the same way.

   Section 3.2 was modified to better explain these aspects of the design.

4. *[**Reviewer**] Why the radius increase was fixed to 5%? Perhaps it would be preferable to leave the radius a free parameter in the optimization and find the optimum radius for every configuration. Perhaps in this way you could better exploit the mass reduction of the downwind coning concept by increasing as much as possible the energy yield.*

   [**Authors**] It is true that a more rigorous approach would consist of a complete redesign of the machine, where among other optimization variables the rotor radius should be left free to minimize the CoE. This is indeed the approach followed in other works that

adopted the same optimization framework, such as Bortolotti et al., 2016[4] and Bortolotti et al., 2018[5].

A simplified approach as the parametric study reported in the present paper is however considered to be more useful at this stage. A change in the rotor radius causes massive changes in all parameters of the turbine, and the interpretation of the results of an automatic optimization may rapidly become challenging. Instead, a pre-defined exploration of the solution space does not offer the possibility to identify an optimum configuration, but helps understand the trends and suggests areas of investigation that are worth further design efforts.

This being said, a recommendation for future work in the area of aerostructural optimization of downwind rotors was added to Sect. 4.

5. *[**Reviewer**] It is not clear how would the coning system operate in the case of grid loss especially if this is combined with storm conditions. Analyzing parked operation at 30deg misalignment implies that the yaw system is not active. Would it be possible in this case to cone the blades?*

   [**Authors**] This is a very good point: a grid loss would be extremely problematic for an actively controlled rotor coning such as the one modelled in configuration DW5LA. This aspect was added among the critical ones discussed in Sect. 3.4.

6. *[**Reviewer**] It would be instructive for the reader to know which are the driving DLCs for the different loads. Some information is given in 3.4. Perhaps it would be nice to indicate the DLCs in plot 4b.*

   [**Authors**] We agree with the suggestion and Figure 4b is now split into two distinct figures, showing a list of ultimate and fatigue loads. The ultimate loads are accompanied by the indication of the DLC.

   It is important to notice that this comment of Reviewer 2 not only improved the content of the paper, but also helped spotting a mistake in the paper. In Sect. 3.1 of the original submission, we wrote that the list of DLC included DLC 1.1, 1.3, 2.3 and 6.2. This was a misprint, as DLC 1.3 were not part of the subset of simulations included in this study. The text in Sect. 3.1 has now been corrected.

Minor comments and editorial

1. *[**Reviewer**] Page 2, line 3, add blade prebend*

   [**Authors**] Prebend is added to uptilt and cone angles as a mean to increase tower clearance.

[4] Bortolotti P, Bottasso CL, Croce A. Combined Preliminary-Detailed Design of Wind Turbines. Wind Energy Science, 2016;1:1-18. doi: 10.5194/wes-1-71-2016

[5] Bortolotti P, Bottasso CL, Croce A, Sartori L. Integration of multiple passive load mitigation technologies by automated design optimization—The case study of a medium-size onshore wind turbine. Wind Energy. 2018;1–15. https://doi.org/10.1002/we.2270

2. *[**Reviewer**] Page 5, line 10, you could add any deterministic asymmetry of the inflow and rotational sampling of turbulence*

   [**Authors**] It is absolutely true that deterministic asymmetries of the inflow and rotational sampling of turbulence further complicate load alignment. This is however somehow included in the wind speed change, which results in changes to F_t. We therefore believe that the simplified explanation of Sect. 2.3 can remain the same.

3. *[**Reviewer**] Page 7, line 3, replace "availably" by "available*

   [**Authors**] The misprint is corrected.

We have taken the opportunity to make several small editorial changes to the text, in order to improve readability. A revised version of the manuscript is attached to the present reply, with the main changes highlighted in blue.

Yours sincerely,
The authors

Comparison between upwind and downwind designs of a 10 MW wind turbine rotor

Pietro Bortolotti, Abhinav Kapila, and Carlo L. Bottasso
Wind Energy Institute, Technische Universität München, D-85748 Garching, Germany
Correspondence to: Carlo L. Bottasso (carlo.bottasso@tum.de)

Abstract. The size of wind turbines has been steadily growing in the pursuit of a lower cost of energy by an increased wind capture. In this trend, the vast majority of wind turbine rotors has been designed based on the conventional three-bladed upwind concept. This paper aims at assessing the optimality of this configuration with respect to a three-bladed downwind design, with and without an actively controlled variable coning used to reduce the cantilever loading of the blades. Results indicate that a conventional design appears difficult to beat even at these turbine sizes, although a downwind non-aligned configuration might be an interesting alternative.

1 Introduction

The size of wind turbines in terms of both rotor diameter and nameplate power has been dramatically increasing over the last few decades. The key driver behind this spectacular growth has been the reduction in levelized cost of energy (CoE), which typically benefits from an increase in energy capture. The trend is expected to continue as more countries promote new offshore installations and onshore wind increases its presence in regions of low average wind speeds. In addition, in countries characterized by a high penetration of wind power such as Denmark and Germany, the structure of the electricity market tends to favor larger rotor sizes. In fact, the price of electricity in these markets is increasingly correlated with the availability of wind power. At times when wind power is abundant, electric grids may experience an excess of power generation, which in turn leads spot market prices to markedly drop (Badyda and Dylik, 2017), ultimately reducing the importance of power production in high winds.

The growth in rotor diameters is however pushing the limits of conventional wind turbine configurations. For example, one especially important design driver of very long blades is the minimum clearance between tip and tower to prevent strikes. In fact, the design of large upwind rotors is often driven by tip-clearance requirements (Bortolotti et al., 2016, 2018). To meet this constraint, designers are increasingly adopting a combination of thick airfoils and high-modulus composites to increase the out-of-plane stiffness of the blades. Together with an increase in blade prebend, rotor cone and nacelle uptilt angles, these design choices help satisfying the tower clearance constraint. Nonetheless, achieving CoE reductions by upscaling conventional upwind configurations is an increasingly challenging task.

In this scenario, the recent literature suggests that downwind rotor configurations may offer the opportunity to generate lower CoE values compared to traditional upwind ones (Frau et al., 2015). Cost reductions could be obtained in downwind

configurations thanks to lighter and more flexible blades, made possible by a relaxed tower clearance constraint. In addition, an increased AEP could be generated by reduced cone and uptilt angles, as well as by a favourable blockage effect generated by the nacelle. In fact, the presence of the nacelle located upwind of the rotor has the effect of redirecting the flow towards the outboard part of the blade. This way, the flow speeds up towards blade sections characterized by thinner and more efficient airfoils and, as a result, a higher AEP is produced. An experimental campaign on sub-scale models showed an increase in AEP equal to 5% against an increase of 3% of rotor thrust (Kress et al., 2015a). Furthermore, in sites characterized by upflow angles, such as hills and ridges, the uptilt angle improves the alignment of the rotor with the incoming wind in the downwind case, while it has the opposite effect in the upwind one. Lastly, the weathercock stability of downwind rotors could, at least in principle, be exploited to reduce the cost of the yaw system (Kress et al., 2015a).

Clearly, these benefits would not come for free, and downwind rotors struggle against a major disadvantage, namely an increased tower shadow effect (Reiso, 2013). This results into two main negative effects compared to equivalent upwind designs. First, fatigue loading typically increases due to a higher one-per-revolution harmonic blade excitation (Manwell et al., 2009; Kress et al., 2015b). Secondly, higher noise emissions are generated due to the blade interference with the tower wake, especially in the low frequency range of the noise spectrum (Madsen et al., 2007). These two aspects have been especially important for early onshore machines and, as a result, most modern designs worldwide adopt the upwind configuration. One notable exception to this situation is represented by the downwind machines developed by Hitachi Ltd. and installed in Japan (Kress et al., 2015b).

An additional potential advantage of downwind rotors is the possibility of achieving the so called "load alignment" along the blades, a novel concept proposed and investigated in Ichter et al. (2016); Loth et al. (2017); Noyes et al. (2018). Load alignment may be seen as bio-inspired by palm trees, which sustain storms by bending downwind and aligning their leaves in the wind direction. In turn, this has the effect of turning cantilever loads into tensile ones. In Ichter et al. (2016); Loth et al. (2017); Noyes et al. (2018) this concept is investigated by designing a 13.2 MW two-bladed downwind rotor, which exhibits a decreased CoE in comparison to an equivalent upwind three-bladed configuration. This claim is supported by reduced out-of-plane fatigue and ultimate loads that lead to a reduction of blade mass.

Goal of this work is the comparison of three-bladed upwind rotor configurations with three-bladed downwind designs, including load alignment. The present work does not consider the case of teetering two-bladed rotors. The novelty of the present investigation resides in the fact that, differently from the existing literature, each wind turbine design is subjected to a detailed aerostructural optimization to minimize its CoE. The comprehensive design procedures used here account for all necessary design constraints and consider the various multi-disciplinary couplings of the problem, which are necessary to identify CoE-optimal constraint-satisfying solutions. This is achieved by balancing turbine capital cost and annual energy production (AEP). Examples of publicly available design frameworks include `HAWTOpt2` (Zahle et al., 2016), `WISDEM` (Dykes et al., 2014) and `Cp-Max` (Bortolotti et al., 2016, 2018), the latter being used for the present investigation.

The design optimization procedures are driven by the combination of two cost models. A first model developed at Sandia National Laboratories (Johans and Griffith, 2013) is used to estimate the blade cost. This model overcomes the use of simplified relationship between blade mass or blade length versus blade cost, and it accounts for material, equipment and labor costs. CoE

is estimated by the cost model developed within the INNWIND.EU project (INNWIND.EU, Deliverable 1.23 , 2014). This second cost model is especially focused on next-generation offshore wind turbine designs.

The presentation is structured as follows. Section 2 reviews the aeroservoelastic simulation models used in the study, the load alignment concept and a short summary of the aerostructural design procedures. Then, Sect. 3 discusses the wind turbine configuration used as baseline and the novel downwind designs, which are compared in terms of loads, performance and costs. The study is closed in Sect. 4, where the main conclusions of the study are summarized.

2 Modeling, simulation and design

This work is concerned with the evaluation of design configurations of wind turbines. This activity is supported by the wind turbine design framework `Cp-Max`, which uses aeroservoelastic models implemented within the wind turbine simulator `Cp-Lambda` coupled to a model-based controller, which are described in Sect. 2.1 and 2.2, respectively. This background information is followed by Sect. 2.3, where the load alignment design concept is reviewed. Finally, Sect. 2.4 briefly recalls the design procedures implemented in `Cp-Max`.

2.1 Aeroelasticity

The aeroelastic behavior of the various wind turbine design configurations is computed in this work with the aeroservoelastic simulator `Cp-Lambda` (Code for Performance, Loads and Aeroelasticity by Multi-Body Dynamic Analysis). `Cp-Lambda` implements a multi-body formulation for flexible systems with general topologies and features a library of elements, which includes rigid bodies, non-linear flexible elements, joints, actuators and aerodynamic models (Bottasso et al., 2006; Bauchau, 2011). Sensor and control elements enable the implementation of generic control laws. The multi-body index-3 formulation is expressed in terms of Cartesian coordinates, while constraints are enforced by scaled Lagrange multipliers. In this study, the rotor blades and the tower are modeled by non-linear geometrically-exact shear and torsion-deformable beam models. Fully populated stiffness matrices account for couplings generated by anisotropic composite materials. Flexible components are discretized in space, leading to a system of differential algebraic equations in the time domain.

The blade aerodynamic characteristics are defined by lifting lines, which include the spanwise chord and twist distributions as well as sectional aerodynamic coefficients, given in tabular form and parameterized in terms of Reynolds number. The calculation of aerodynamic loads is performed at selected points, called air stations, along each lifting line. Each air station is rigidly connected to an associated beam cross-section, and moves with it. As a consequence, the local airflow kinematics at each air station include the contributions due to blade movement and deformation. In addition, the effects of the wake are modeled by a classical Blade-Element Momentum (BEM) model based on annular stream tube theory with wake swirl and unsteady corrections (Hansen, 2008), or by the dynamic inflow model of Pitt and Peters (1981); Peters and He (1995). The aerodynamic description is completed by root and blade tip losses, unsteady aerodynamic corrections, dynamic stall, 3D blade root delayed stall and upwind and downwind rotor-tower interference models. For upwind rotors, the tower shadow effect is modeled by assuming an incompressible laminar flow around a cylinder, while the model of Powles (1983) is used in the

downwind case. No dedicated nacelle blockage model is instead included in the simulation of downwind configurations, which might lead to a slight underestimation of power capture.

A parameterized model of the blade structure is defined by choosing a number of control stations. At each section of interest, airfoils, blade topology, composite mechanical properties and the geometry of the cross section structural members are given, and the cross sectional solver `ANBA` (Giavotto et al., 1983) is used to produce the associated six-by-six stiffness matrix and sectional blade properties. In turn, these properties are used to define the corresponding beams in the `Cp-Lambda` model.

2.2 Model based controller

The virtual wind turbines developed in this study are governed over their entire operating range by a controller interfaced with `Cp-Lambda` through external dynamic libraries. A supervisory unit manages the machine behavior by switching among different operating states and handling emergencies. Pitch and torque are handled by suitable controllers operating in closed-loop with the machine on the basis of data supplied by sensor models. All wind turbine models developed in the current study use the linear quadratic regulator (LQR) described in Bottasso et al. (2012). This model-based formulation allows for a straightforward update of the control laws during design, as its underlying reduced-order model can be readily updated whenever the wind turbine parameters change, thereby automatically producing new sets of gains that work in combination with the new design. While probably not superior to other classical pitch-torque controllers used in industrial practice, this method is found to be useful in this research context as it allows for an automatic tuning of the control laws throughout the design process.

The LQR controller is synthesized by means of simulations run in steady wind conditions to evaluate the aerodynamic performance of the machine for a three-dimensional grid of tip speed ratios λ, blade pitch angles β and wind speeds V. These simulations take into account the aeroelastic effects of the flexible bodies of the entire wind turbine model and include the computation of aerodynamic, inertial and gravitational loads. The aerodynamic performance is evaluated by extracting internal forces at the hub, which yield the thrust force and shaft torque. By non-dimensionalizing these values, one obtains the thrust C_T and power C_P coefficients, as functions of λ, β and V, which are stored in look-up tables. Based on the C_P tables, the regulation trajectory of the machine is computed, defining the control parameters (pitch, rotational speed and torque) for regions II and III, defined as the operating regions between cut-in wind speed V_{in} and rated wind speed V_{r}, and between V_{r} and cut-out wind speed V_{out}, respectively (Bottasso et al., 2012). In region II, C_P is maximized, while in region III power is held constant. In addition, the rotor is regulated to comply with a possible limit on the maximum blade tip speed, which may result in the appearance of a transition region II½ in between the partial and full loading regimes.

2.3 Load aligned rotor

The concept of load alignment for wind turbine rotors has been introduced and developed in Ichter et al. (2016); Loth et al. (2017); Noyes et al. (2018). The idea consists of designing a suitably pre-bent blade in order to align the resultant of the various forces acting on the blade with its axis. The goal of such alignment is to convert out-of-plane cantilever forces into tensile ones, which can be resisted by a lighter weight structure.

The primary forces acting on a wind turbine rotor are the thrust force F_t, centrifugal force F_c and gravitational force F_g. Since F_t greatly depends on the wind speed and F_c on the rotational speed, which in turn depends on the wind speed as well, the force resultant changes magnitude and direction over time. An exact load alignment can then be achieved only by a truly morphing blade that adjusts its out-of-plane shape based on wind speed. In this study, the prebent shape of the blade is instead assumed to be frozen, while an out-of-plane load alignment at blade root is sought by means of three flap hinges and three corresponding actuators. Goal of hinges and actuators is to actively control the cone angle γ of each blade. Figure 1 shows a schematic view of this concept.

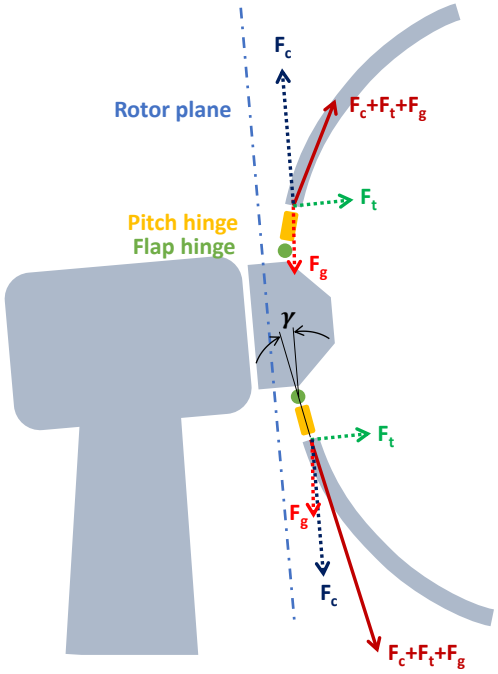

Figure 1. Schematic view of the active load alignment concept.

The resultant of the three forces F_t, F_c and F_g does not only depend on wind speed, but also changes its direction with the azimuthal position of the blade. This change is caused by the periodic variation of the gravitational loading F_g acting on the rotating blade, and by the atmospheric wind shear influencing F_t. As a result, an exact load alignment at blade root can only be achieved by an individual control of the angle γ for each one of the blades. This would however require a flap actuator control rate of several degrees per second. In addition, individual flapping of the blades would break the rotor axial symmetry, generating major rotor mass imbalances. Because of these reasons, an average (collective) γ is used for the three blades, which is changed based on wind speed. A maximum value is set for the blade root out-of-plane moments across one whole rotor revolution. When this threshold value is exceeded, the rotor blades are collectively coned by an angle γ. The coning value is chosen based on a 30-second moving average of the wind speed, which removes fast fluctuations and aims at identifying

the current mean operating condition. To avoid inaccuracies of the nacelle anemometer, a rotor-equivalent wind speed may be obtained by a suitable estimator (Soltani et al., 2013).

2.4 Blade aerostructural design optimization

`Cp-Max` implements wind turbine design methods that integrate a blade aerodynamic optimization with a blade and tower structural optimization, within an overall turbine optimization procedure. The optimization loops are structured following a nested architecture and the overall design goal is the minimization of the CoE. In this study, only the aerodynamic and the structural optimization loops of the blade are used, while the tower is held frozen. For a more complete overview of the design methodologies implemented in `Cp-Max`, interested readers can refer to Bortolotti et al. (2016) and references therein.

The aerodynamic optimization loop is used here to compute an optimal twist distribution for all designed blades. However, the planform shape of all blades was kept the same of the baseline design. Twist is parameterized along the blade span at a number of stations. In each station, an optimization variable is defined, corresponding to an additive gain added to the local twist. The actual twist distribution is reconstructed by means of Piecewise Cubic Hermite Interpolating Polynomial (PCHIP) splines. The merit figure of the aerodynamic optimization is the maximization of AEP, while linear and non-linear constraints are appended to the problem to specify all necessary design requirements and desired features.

The structural optimization aims at the sizing of the blade inner structure for a given outer blade shape. The optimization consists of an iterative loop, beginning with the calculation of the regulation trajectory and the synthesis of the LQR controller gains, which are updated based on the current wind turbine design (Bottasso et al., 2012). Next, a load computation step is performed where a list of design load cases (DLCs) is run. The post-processed results of these analyses are used to compute the load envelopes at a number of verification stations along the three blades. The rainflow counting required to estimate fatigue damage is also performed here. Given these inputs, the actual structural sizing is computed by means of a sequential quadratic programming (SQP) algorithm, which is well suited to problems with several constraints that are potentially simultaneously active at convergence. The merit figure of the structural sizing step is blade cost, which is calculated from the SANDIA blade cost model. Gradients are computed by means of forward finite differences. Once the solver converges to a new blade structure, the process iterates back to the tuning of the LQR controller and all steps are repeated until blade cost converges to a pre-defined tolerance, which is usually set at 1%.

3 Comparison of design configurations

In this section, the baseline upwind model used as benchmark is first presented in Sect. 3.1. Then, Sect. 3.2 reviews the downwind design configurations developed from the baseline. These are finally compared in Sect. 3.3 in terms of loads, blade mass, blade cost, AEP and CoE. Finally, some critical aspects of the load aligned solution are discussed in Sect. 3.4.

3.1 Baseline model

The DTU 10 MW reference wind turbine (RWT) platform is here chosen as a significant test case. This wind turbine is a conceptual machine developed by the Wind Energy Department of Denmark Technical University (DTU), freely available in the public domain for research purposes. The main characteristics of the wind turbine are reported in Table 1, while a more complete description of the model and the criteria used for its design are given in Bak et al. (2013). In this study, the blade prebend distribution is optimized with `Cp-Max` following Sartori et al. (2016), which resulted in the solution reported in Fig. 2. Given this prebend, the blade twist and internal structure are updated by the aerostructural design optimization described in Sect. 2.4, while keeping the planform shape unchanged. For simplicity, a reduced set of DLCs is used, namely DLC 1.1, 2.3 and 6.2. These represent normal operating conditions, the occurrence of extreme gusts combined with electric faults and the occurrence of a 50-year storm at twelve different values of yaw angle (IEC, 2005). To reduce the computational cost, a single seed per wind speed is used in the turbulent cases, namely DLC 1.1 and DLC 6.2. Although this means that the estimation of fatigue loading and AEP might not be fully converged, it still allows for meaningful comparisons, as the same wind time history for each wind speed was used for all designs.

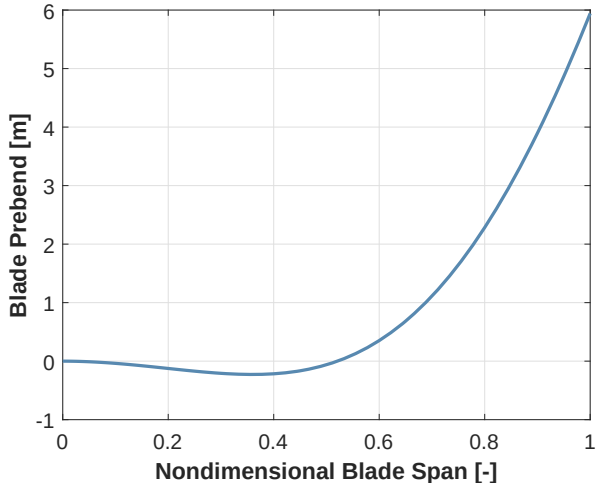

Figure 2. Prebend distribution obtained by `Cp-Max` during the redesign of the 10 MW DTU RWT.

Table 1. Main parameters of the DTU 10 MW RWT.

Data	Value
Wind class	IEC 1A
Rated electrical power	10 MW
Cut-in wind speed V_{in}	4 m/s
Cut-out wind speed V_{out}	25 m/s
Rotor diameter	178.3 m
Hub height	119.0 m

The blade inner configuration is a fairly standard spar box construction, except for the presence of a third shear web running along part of the blade span close to the trailing edge. Unidirectional fiberglass reinforcements are located at the leading and trailing edges, while an additional reinforcement is superimposed to the external shell in the blade root region. Table 2 reports the spanwise extension of the structural components and their materials. Transversely isotropic laminae are assumed to have the characteristics summarized in Table 2. The mechanical properties of the resulting composites are computed by classical laminate theory.

Table 2. Extent of the structural components and their materials in the blade of the 10 MW wind turbine.

Component	From (% η)	To (% η)	Material type	Longitudinal Young's modulus [MPa]	Transversal Young's modulus [MPa]	Shear modulus [MPa]
Spar caps	1	99.8				
LE-TE reinforcements	10	95	Uni-dir. GFRP	41,630	14,930	5,047
Root reinforcement	0	45				
First and second shear webs skin	5	99.8	Bi-axial GFRP	13,920	13,920	11,500
External shell	0	100	Tri-axial GFRP	21,790	14,670	9,413
Third shear web skin	22	95				
Shell and webs core	5	99.8	Balsa	50	50	150

3.2 New configurations

The original upwind configuration (UW) is adopted as the starting point to establish a comparison amongst various alternatives:

a) UW5: upwind redesign with a 5% larger rotor diameter;

b) DW: downwind design;

c) DW5: downwind redesign with a 5% larger rotor diameter;

d) DW5LA: downwind redesign with active load alignment and a 5% larger rotor diameter.

From a multi-body modeling point of view, configurations UW, UW5, DW and DW5 have exactly the same topological structure, where the only differences lay in the orientation of the rotor and the presence of actuated flap hinges for the active coning solution of DW5LA, as discussed in Sect. 2.3. The aeroelastic models also differ in the tower shadow effect (downwind or upwind) and in the length of the blades. The hub is identical among the five configurations, while the blade external shapes in UW5, DW5 and DW5LA are geometrically scaled from UW, resulting in rotors with the same solidity and hence also the same tip-speed-ratio for maximum power coefficient. The use of a fixed increase in diameter (5%) for all rotors is meant to highlight the trend of the solution for a given assigned change. An alternative approach might have been to optimize the rotor diameter in order to increase power capture while not exceeding the loads of the baseline design, as done for example in Bortolotti et al. (2016) and Bortolotti et al. (2018).

Regarding DW5LA, it was observed that out-of-plane blade root moments cannot be reduced to zero, as this would require a flap angle γ in excess of 45 deg at rated wind speed. This would lead to a dramatic reduction of the rotor swept area and,

consequently, of the generated AEP. After several tests, it was decided to limit the out-of-plane moment at blade root to 50% of the maximum steady state value measured in the UW design, namely 22 MNm. The resulting scheduled values of γ are reported in Fig. 3a, where the angle magnitude is visibly influenced by F_t. Between V_{in} and V_{r}, the prescribed γ is first held at 0 deg, since the out-of-plane moment at blade root is below the threshold of 22 MNm. Above a wind speed of 9 m/s, the prescribed γ rapidly increases until rated conditions following the increase in F_t, but keeping the out-of-plane moment at blade root below 22 MNm. Above V_{r}, blades are pitched into the wind, which results into a reduction of F_t and, consequently, also of γ.

Tests were also conducted to determine a suitable choice for the coning rate $\dot{\gamma}$. Different values of this parameter from 0.001 deg/s to 1 deg/s were tested in DLC 1.1, analyzing the resulting out-of-plane blade root moment, as reported in Fig. 3b. Although lower values of $\dot{\gamma}$ could probably be sufficient, a minimum of the loads is identified at 0.25 deg/s, which is the value used for the DW5LA design.

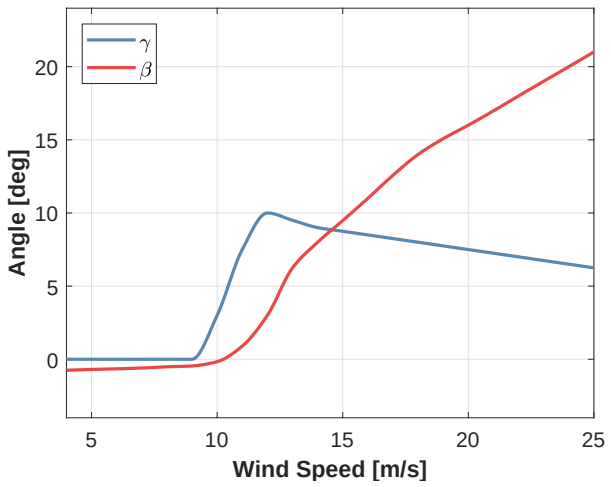

(a) Cone γ and pitch β angles vs. wind speed for DW5LA.

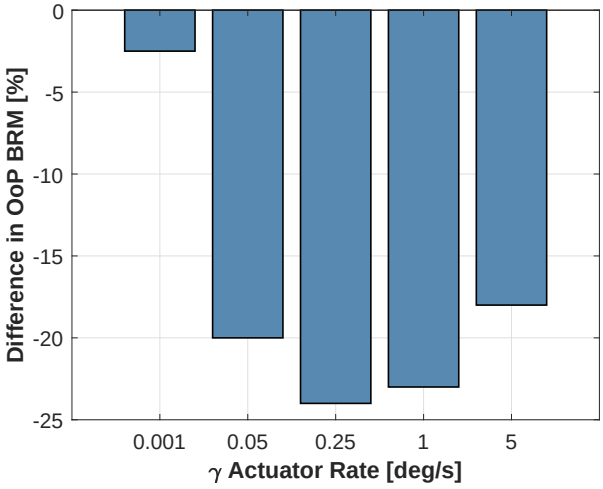

(b) Effect of γ rate on maximum out-of-plane moment measured at blade root in DLC 1.1.

Figure 3. Cone and cone rate for the DW5LA design.

All five configurations were then subjected to an aerodynamic optimization of the twist and a blade structural optimization, as described in Sect. 2.4. Once the two loops converge, the AEP and the CoE are evaluated. The comparison in terms of cost and performance is discussed next.

3.3 Cost and performance comparison

A comparison among the five configurations is presented with the histogram shown in Fig. 4a. First, as already observed in Bortolotti et al. (2016), the current cost models predict a reduction of CoE when the rotor is enlarged. Within this trend,

downwind configurations appear to be able to successfully limit the growth in blade mass and cost. This effect is generated by the relaxed tower clearance constraint, which is instead a critical design driver for the UW and UW5 designs. It is however interesting to highlight that, although smaller than in the upwind cases, high blade deflections also occur in DW and DW5 during the emergency shutdowns simulated with DLC 2.3. Possibly, optimized shutdown maneuvers could help in generating further mass and cost reductions, but a dedicated study would be needed to more precisely quantify any saving. Although costs are reduced, DW and DW5 generate smaller values of AEP compared to UW and UW5. These reductions are mostly caused by an increased flexibility of the blades, which bend when loaded, in turn reducing the rotor swept area. For a given rotor cone angle, this effect is more detrimental for downwind rotors compared to an equivalent upwind one, as cone and prebend are against the wind in the latter case. The comparison is instead different as soon as an upflow is present in the incoming wind, which is the typical case of complex terrain conditions when the turbine is located on a hill or close to a ridge. In the present case, an upflow of 5 deg changes the trend and increases the AEP of the downwind rotors by 0.7% with respect to their upwind equivalents. This higher AEP is directly converted into a reduction of CoE for both DW and DW5. Notably, changes in AEP are only modest, especially when considering the variety of uncertainties affecting wind turbine simulations. Nonetheless, it should be remarked that a variation 0.7% in AEP is not completely negligible, as the two rotors are characterized by the same diameter, they are both optimized in terms of twist and control gains, and they are both subjected to the same wind of class I (where the contribution of region III to AEP is not marginal). In addition, the trend is consistent between the rotors with the baseline diameter, namely UW and DW, and the rotors with the longer blades, namely UW5 and DW5. Finally, tests conducted in steady-state wind conditions corroborate these results. It may be useful to remind that, as mentioned earlier on, nacelle blockage is not accounted for in the simulation models, and its inclusion might generate slight benefits in AEP for DW and DW5. In this scenario, DW5LA has a lower blade mass and cost compared to UW5 and DW5, but also a slightly lower AEP.

A load assessment is then conducted looking at key ultimate and fatigue loads measured at blade root and at the hub. The comparison is reported in Fig. 4b and Fig. 4c. In terms of flapwise blade root moments (FBRM), downwind configurations DW and DW5 help in reducing ultimate loads, while generating approximately the same fatigue loading. On the other hand, DW5LA reduces both ultimate and fatigue loads compared to UW5 and DW5. For the edgewise blade root moment (EBRM), fatigue loads follow the blade mass trend. In the case of fatigue torsional blade root moments (TBRM), an alarming growth is observed for DW5LA. This is due to the increased out-of-plane deformations induced by a decreased blade stiffness. At the hub, trends are more scattered, with a decrease of the ultimate thrust (ThH) for DW and DW5LA, but an overall marked increase of ultimate out-of-plane bending moments (OoPMH), especially for DW5LA. Finally, the tower base fore-aft (TBFA) moment of DW, DW5 and DW5LA sees a decrease in its ultimate value, but an increase in fatigue except for DW5LA, which stays approximately constant. Notably, ultimate TBFA are generated in operational conditions for UW and UW5, shutdown conditions in the case of DW and finally storm conditions for DW5 and DW5LA.

Overall, DW and DW5 are associated with generally lower loading compared to UW and UW5, except for ultimate OoPMH and fatigue TBFA. Larger TBFA may generate an increase in the mass and cost of a steel tower, which is often fatigue-driven (Bortolotti et al., 2018). DW5LA is instead effective in reducing loads aligned with the prevailing wind direction, namely FBRM, ThS and TBFA. Furthermore, it benefits from a decreased blade mass and stiffness that result into lower EBRM. This

is however obtained at the cost of increased torsional moments on the blades (which would impact the pitch system design), and out-of-plane moments at the hub (which would impact the design of the shaft and of the main bearings). A specific, more detailed, design activity would be necessary to more precisely quantify these effects. In addition, DW5LA is prone to several critical aspects, which are assessed in Sect. 3.4.

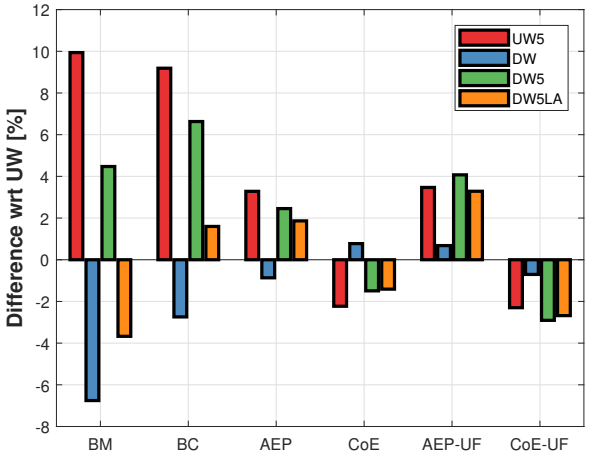

(a) Figures of merit.

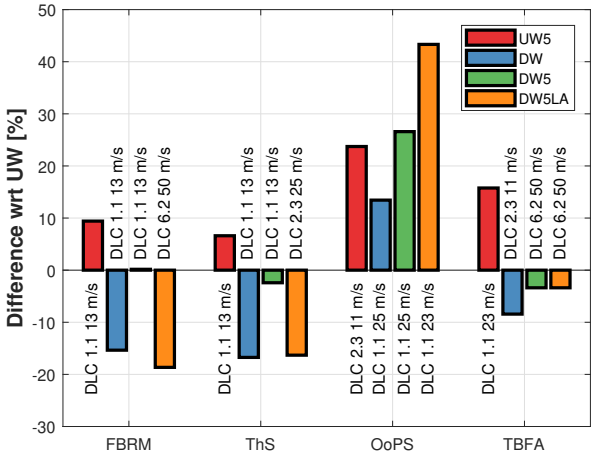

(b) Ultimate loads and corresponding DLC.

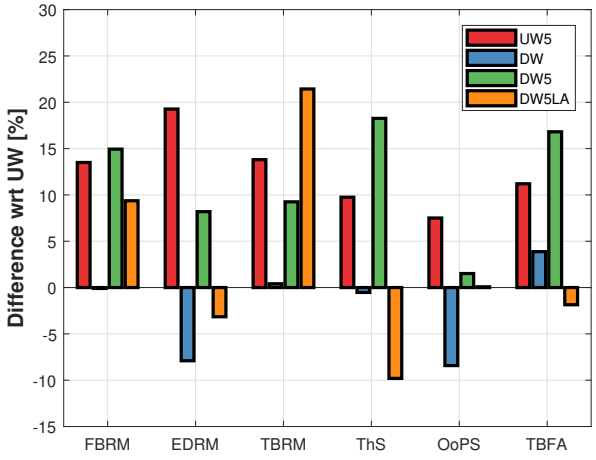

(c) Fatigue loads.

Figure 4. Comparison in terms of main figures of merit (a), ultimate (b) and fatigue loads (c) for the four designs with respect to the baseline configuration UW. The CoE of DW5LA does not include in the calculations the capital cost and power consumption of the active coning system. Legend — BM: blade mass; BC: blade cost; UF: 5 deg of upflow; FBRM-EBRM-TBRM: flapwise, edgewise and torsional blade root moments; ThH-OoPMH: thrust and out-of-plane moment at the hub; TBFA: tower base fore-aft moment. In (b), the dominating DLCs of UW are the same of UW5.

3.4 Critical aspects of DW5LA and comparison with the literature

As shown in Fig. 5a, compared to configuration DW5, power losses of the design solution DW5LA are limited to wind speeds around rated conditions. However, active load alignment in turbulent dynamic cases is only partially effective. In fact, although blade root moments do indeed decrease thanks to active coning, moments at other points along the blade span are not significantly affected. It is speculated that a reduction of moments throughout a larger portion of blade span would necessitate of a truly morphing solution, with adjustable prebend. As a result of the only partial effectiveness of active coning, the blade cost of DW5LA is not significantly reduced compared to the one of configuration DW5. In addition, loads generated during storm conditions are not necessarily alleviated by active coning. In fact, folding the rotor will reduce its swept area, but it will also dramatically move the rotor center of gravity away from the tower, resulting in very large loading of the structure and foundations. For example, aeroelastic simulations were performed in storm conditions with a wind misaligned by ± 30 deg, having folded the blades with a value of $\gamma = 60$ deg. Although a more sophisticated CFD analysis would be needed to accurately predict aerodynamic forces at such angles of attack, bending moments at the hub were doubled, while tower base moments increase by 40%.

Finally, for the chosen coning rate $\dot{\gamma}$ the actuators of configuration DW5LA have a non negligible power consumption. Figure 5b shows the consumption estimated during DLC 1.1 for the case without a power recovery system (label woRec) and with a recovery system having an efficiency of 80% (label wRec). Such solution, although technologically complex, would be able to recover most of the energy used by the actuators.

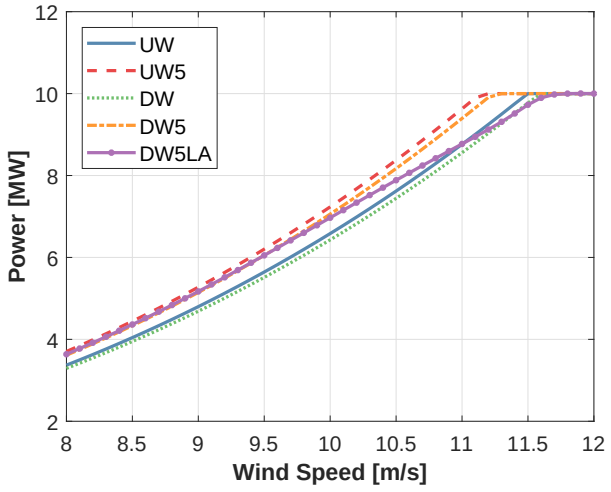

(a) Comparison of power curves.

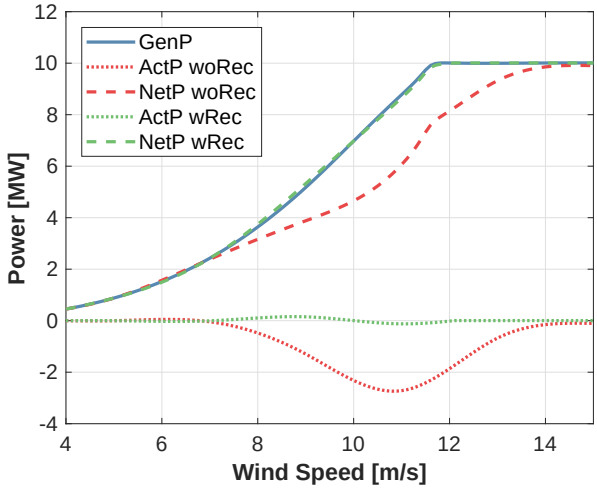

(b) Power curves for DW5LA.

Figure 5. Power generation for the five designs (left) and power consumption of the three coning actuators with and without recovery system (wRec and woRec, respectively). The efficiency of the recovery system is assumed to be equal to 80%.

Overall, given the fact that the joints and actuators necessary for active coning would certainly pose serious engineering challenges and associated costs, a conventional downwind configuration would appear here to be more interesting than an actively load-aligned one.

This conclusion is somewhat less promising than the ones presented in Ichter et al. (2016); Loth et al. (2017); Noyes et al. (2018). Two aspects may explain these differences. First, simplified analyses were conducted in the cited references, using steady-state conditions and no shutdown nor storm load cases, performing only a preliminary structural analysis. Secondly, the results presented in the literature adopt different design assumptions, including a two-bladed rotor with a constant γ (set to 17.5 deg). In this work, the use of a constant γ was attempted, but proved to be ineffective for the current 10 MW case because of a dramatic reduction in AEP and of a limited load alignment capability. In addition, a sufficiently high value of the coning rate appears to be necessary in highly turbulent wind conditions, such as the ones of the class 1A DTU 10 MW RWT considered here. These design choices differ from the ones assumed in the literature and, together with the arbitrary setting of the maximum blade root moment to 22 MNm, may affect the conclusions.

Finally, a variable coning mechanism may raise major concerns in the presence of flap angle misalignments among the blades (for example, because of faults in one actuator or encoder), which could cause problematic rotor imbalances. Additionally, the case of partial or total power loss at the actuators should also be addressed and satisfactorily solved to ensure safety.

4 Conclusions and future work

This paper has presented a comparative study among five three-bladed upwind and downwind wind turbine configurations, with the aim of investigating the potential merit of downwind solutions and active load alignment in a 10 MW case. Based on the results reported herein, the following main conclusions can be drawn together with recommendations for future work.

4.1 Conclusions

First, downwind rotors help in limiting mass and cost of very large blades. Specifically, results indicate reductions of 6% in mass and 2% in cost. It is speculated that further benefits could be obtained by optimized ad-hoc shutdown strategies. In addition, when the atmospheric flow is characterized by an upflow, such as in some complex terrain conditions, downwind machines generate a higher AEP than equivalent upwind designs because of a more favorable attitude of the rotor with respect to the incoming wind. In this study, a downwind rotor operating in a wind with an upflow of 5 deg generates 0.7% more AEP than an equivalent upwind configuration. Any such increase, together with savings in blade cost, can lead to CoE reductions at approximately the same loading.

Secondly, generating an effective load alignment in highly turbulent wind conditions and storms appears to be a non-trivial task, even with an active solution. In addition, losses in AEP compared to traditional downwind designs are observed. These effects negatively impact the CoE. The power consumed by the three coning actuators is also non negligible, peaking for the configuration analyzed here at a staggering average of nearly 3 MW around rated wind speed. Without a power recovery system, this would dramatically impact the AEP. The extra investment for the three actuators, both in terms of capital and

operational cost, is also expected to significantly impact the CoE. Finally, during storms, the usefulness of load alignment is very questionable, as the folding of a large rotor is unrealistic due to the resulting dramatic increase of hub and tower base moments.

Overall, conventional (non-coning) downwind designs are found to be more promising. These configurations could offer advantages either in conditions of marked atmospheric upflow or in case of very large offshore machines, where blade mass needs to be limited. Having said this, it should also be remarked that the standard upwind solution appears to be very difficult to beat, even at these large sizes. Given the very significant body of knowledge and experience on this configuration accumulated by industry so far, it remains to be seen whether the advantages of downwind solutions are worth the effort and risk that are undoubtedly necessary to bring them to full maturity.

4.2 Recommendation for future work

Additional investigations are necessary to address the assumptions and design decisions that may affect the conclusions of this work. For the comparison among UW, UW5, DW and DW5, an assessment of the effects of the four rotors on the design of the tower and of the nacelle components should be conducted. In addition, the blockage effect generated by the nacelle, which is not included in the present analysis, could possibly slightly improve the AEP and CoE of the downwind configurations. In this context, it would be useful to develop analytical corrections for BEM-based models to account for the presence of the nacelle in a downwind rotor. Furthermore, it is recommended to increase the number of turbulent seeds and possibly run the full list of DLCs as prescribed by international standards (IEC, 2005). Special attention should be given to the case of complex terrain installations. As suggested by Kress et al. (2015a) and by the results reported in this paper, a downwind configuration may benefit in terms of AEP. However, an especially careful load assessment should be conducted as complex terrain conditions may also be characterized by increased unsteadiness in the wind, high shear and recirculation regions, which may result in higher loads on the turbine. Finally, a more rigorous holistic design optimization for upwind and downwind configurations should be conducted, including an optimization of the rotor diameter.

Regarding the active coning solution, additional studies should assess the optimality of the design assumptions made so far, focusing especially on the amount of blade prebend, on the maximum flapwise blade root moment and on the coning rate. Finally, a more complete comparison with the existing literature should also consider the development of a teetering two-bladed downwind rotor, which was not studied here and might significantly change the conclusions.

Acknowledgements. The authors gratefully acknowledge the partial financial support of the ICER TUM-NTU project, directed by Prof. Subodh Mhaisalkar and Prof. Thomas Hamacher.

References

Badyda K, Dylik M. Analysis of the Impact of Wind on Electricity Prices Based on Selected European Countries. *Energy Procedia*, 2017;105:55-61. doi: 10.1016/j.egypro.2017.03.279

Bak C, Zahle F, Bitsche R, Kim T, Yde A, Henriksen LC, Andersen PB, Natarajan A, Hansen MH. Description of the DTU 10 MW reference wind turbine. *DTU Wind Energy Report-I-0092*, July, 2013.

Bauchau OA. Flexible Multibody Dynamics. Mechanics and Its Applications. *Springer*, 2011. ISBN: 978-94-007-0335-3

Bortolotti P, Bottasso CL, Croce A. Combined preliminary-detailed design of wind turbines. *Wind Energy Science*, 2016;1(1):71-88. doi: 10.5194/wes-1-71-2016

Bortolotti P, Sartori L, Croce A, Bottasso CL. Integration of multiple passive load mitigation technologies by automated design optimization - The case study of a medium-size onshore wind turbine. *Wind Energy*, 2018;1–15. doi: 10.1002/we.2270

Bottasso CL, Croce A, Savini B, Sirchi W, Trainelli L. Aero-servo-elastic modeling and control of wind turbines using finite-element multi-body procedures. *Multibody System Dynamics*, 2006;16(3):291-308. doi: 10.1007/s11044-006-9027-1

Bottasso CL, Croce A, Nam Y, Riboldi CED. Power curve tracking in the presence of a tip speed constraint. *Journal of Renewable Energy*, 2012;40:1-12. doi: 10.1016/j.renene.2011.07.045

Bottasso CL, Bortolotti P, Croce A, Gualdoni, F. Integrated aero-structural optimization of wind turbine rotors. *Multibody System Dynamics*, 2016;38(4):317-344. doi: 10.1007/s11044-015-9488-1

Dykes K, Ning A, King R, Graf P, Scott G, Veers P. Sensitivity analysis of wind plant performance to key turbine design parameters: a systems engineering approach, *NREL/CP-5000-60920*, 2014.

Frau E, Kress C, Chokani N, Abhari RS. Comparison of Performance and Unsteady Loads of Multimegawatt Downwind and Upwind Turbines. *Journal of Solar Energy Engineering*, 2015;137(4):041004-041004-8. doi: 10.1115/1.4030314

Giavotto V, Borri M, Mantegazza P, Ghiringhelli G. Anisotropic beam theory and applications. *Computers & Structures*, 1983;16(1-4):403-413. doi: 10.1016/0045-7949(83)90179-7

Hansen MOL. Aerodynamics of Wind Turbines. *2nd edn. Earthscan, London*, 2008. ISBN: 978-1-84407-438-9

Ichter B, Steele A, Loth E, Moriarty P, Selig M. A morphing downwind-aligned rotor concept based on a 13-MW wind turbine. *Wind Energy*, 2016;19(4):625-637. doi: 10.1002/we.1855

INNWIND.EU, Deliverable 1.23, PI-based assessment of innovative concepts (methodology). INNWIND.EU technical report, Deliverable 1.23, April, 2014. Available at: www.innwind.eu

Johans W, Griffith DT. Large Blade Manufacturing Cost Studies Using the Sandia Blade Manufacturing Cost Tool and Sandia 100-meter Blades. *Sandia National Laboratories Technical Report*, 2013.

Janajreh I, Qudaih R, Talab I, Ghenai C. Aerodynamic flow simulation of wind turbine: Downwind versus upwind configuration. *Energy Conversion and Management*, 2010;51(8):1656-1663. doi: 10.1016/j.enconman.2009.12.013

Kress C, Chokani N, Abhari RS. Downwind wind turbine yaw stability and performance. *Renewable Energy*, 2015;83:1157-1165. doi: 10.1016/j.renene.2015.05.040

Kress C, Chokani N, Abhari RS. Design Considerations of Rotor Cone Angle for Downwind Wind Turbines. *ASME. J. Eng. Gas Turbines Power*, 2015;138(5):052602-052602-10. doi: 10.1115/1.4031604

Loth E, Steele A, Qin A, Ichter B, Selig MS, Moriarty P. Downwind pre-aligned rotors for extreme-scale wind turbines. *Wind Energy*, 2017;20(7):1241-1259. doi: 10.1002/we.2092

Noyes C, Qin C, Loth E. Pre-aligned downwind rotor for a 13.2 MW wind turbine. *Renewable Energy*, 2018;116(A):749-754. doi: 10.1016/j.renene.2017.10.019

Madsen HA, Johansen J, Sørensen NN, Larsen GC, Hansen MH. Simulation of Low frequency Noise from a Downwind Wind Turbine Rotor. *45th AIAA Aerospace Sciences Meeting and Exhibit*, Reno, Nevada, 2007. doi: 10.2514/6.2007-623

Manwell JF, McGowan JG, Rogers AL. Wind Energy Explained. *Wiley*, 2009. ISBN: 978-0-470-01500-1

Pitt DM, Peters DA. Theoretical prediction of dynamic inflow derivatives. *Vertica*, 1981;5:21-34.

Peters DA, He CJ. Finite state induced flow models-part II: three-dimensional rotor disk. *J. Aircr.*, 1995;32:323-333. doi:10.2514/3.46719

Powles SRJ. The effects of tower shadow on the dynamics of a HAWT. *Wind Engineering*, 1983;7(1):26-42.

Reiso M. The Tower Shadow Effect in Downwind Wind Turbines. *Ph.D. Thesis*, Norwegian University of Science and Technology, 2013.

Sartori L, Bortolotti P, Croce A, Bottasso CL. Integration of prebend optimization in a holistic wind turbine design tool. *Journal of Physics, Conference Series*, 2016;753. doi: 10.1088/1742-6596/753/6/062006

Soltani MN, Knudsen T, Svenstrup M, Wisniewski R, Brath P, Ortega R, and Johnson K. Estimation of rotor effective wind speed: a comparison. *IEEE T. Contr. Syst. T.*, 2013;21(4):1155-1167. doi:10.1109/TCST.2013.2260751

Wind Turbines Part 1: Design Requirements, Ed. 3. *International Standard IEC 61400-1*, 2005.

Zahle F, Tibaldi C, Pavese C, McWilliam MK, Blasques JPAA, Hansen MH. Design of an Aeroelastically Tailored 10 MW Wind Turbine Rotor. *Journal of Physics, Conference Series*, 2016;753. doi: 10.1088/1742-6596/753/6/062008